




Macrofollicular Architecture in Invasive Encapsulated Follicular Variant of Papillary Thyroid Carcinoma: A Pitfall in Thyroid Practice

Sujata Yadav¹ · Devasenathipathy Kandasamy² · Nishikant Damle³ · Rashi Goel³ · Sunil Chumber⁴ · Mehar C. Sharma⁵ · Monikongkona Boruah¹ · Shipra Agarwal¹ 

Received: 2 August 2023 / Accepted: 9 September 2023 / Published online: 29 September 2023
© The Author(s), under exclusive licence to Springer Science+Business Media, LLC, part of Springer Nature 2023

Abstract

Background Predominantly macrofollicular architecture in invasive encapsulated follicular variant of papillary thyroid carcinoma (IEFVPTC-MF) is rare and often a cause of misinterpretation during pre-operative work-up and histopathology evaluation. We comprehensively evaluated the radiological, cytological, gross, microscopic, molecular and follow-up characteristics of four such cases, intending to increase its recognition and add our experience to the limited literature available.

Methods All such histopathologically-proven cases of IEFVPTC-MF were retrieved from the departmental archives. The clinical details, thyroid ultrasound, cytology and thyroid scan findings were reviewed. Allele-specific PCR for *BRAF* p.V600E, *KRAS*, *NRAS*, and *HRAS* mutations, and FISH assays for *ETV6::NTRK3* fusion and *RET* fusions were performed.

Results There were four cases of IEFVPTC-MF diagnosed between 2021 and 2022, involving two males and two females. The median age at presentation was 27 years, and the duration of the disease was 1–10 years. Thyroid ultrasound was TR1 (benign; $n = 1$), TR2 (not suspicious; $n = 2$), or TR4 (moderately suspicious; $n = 1$). Cytology was categorized as nondiagnostic ($n = 1$), benign ($n = 1$), and atypia of undetermined significance ($n = 1$). The three nodules with available cytology smears showed abundant colloid. Cells were arranged as sheets/microfollicles/clusters. Nuclei were predominantly round with minimal/focal elongation, membrane irregularity, and cellular crowding. On gross examination, cut surfaces of the tumors showed variable amounts of colloid. The tumors were solid-cystic. Histopathology revealed partially encapsulated multinodular tumors. There were prominent pseudopapillae projecting into the lumina of macrofollicles. Nuclei were predominantly round with variable nuclear atypia, including chromatin clearing and multifocal presence of nuclear grooves. Pseudoinclusions were identified in two. Molecular analysis revealed *NRAS* codon 61 mutation and *ETV6::NTRK3* fusion in one case each. Two patients had cervical lymph node and hematogenous metastases. Post-radio-active iodine, the response was structurally incomplete ($n = 2$), indeterminate ($n = 1$) and excellent ($n = 1$).

Conclusions Macrofollicular architecture in invasive encapsulated follicular variant of papillary thyroid carcinoma is a major pitfall in thyroid oncology practice. Long-standing disease, and ultrasonographic and cytological features that overlap with benign disease, often lead to underdiagnosis during pre-operative evaluation. As patients may consequently develop distant metastases and have inadequate treatment response, there is a need for more vigilant understanding of the spectrum of macrofollicular thyroid disease for accurate diagnosis. *ETV6::NTRK3* or other fusions, when found, present opportunities for targeted therapy.

Keywords Macrofollicular invasive encapsulated follicular variant of papillary thyroid carcinoma · IEFVPTC · Cytology · Radiology · Molecular · Thyroid cancer

Introduction

Invasive encapsulated follicular variant of papillary thyroid carcinoma (IEFVPTC) with predominantly macrofollicular architecture, as it is currently recognized was initially

described by Albores-Saavedra in 1991 as a distinctive subtype of PTC. The diagnosis was based upon the presence, at least focally, of the nuclear features of PTC (PTC-N). Of the 17 cases in the series, only five showed capsular invasion [1]. However, as per the 2022 WHO classification of thyroid tumors, a follicular-patterned tumor needs to show invasive features besides PTC-N for characterization as

Extended author information available on the last page of the article

PTC, relegating most of the previously reported entities to a diagnosis of noninvasive follicular thyroid neoplasm with papillary-like nuclear features (NIFTP) [2]. Macrofollicular-patterned tumors can be overtly infiltrative and behave like classic PTC, *BRAFV600E*-like. Alternatively, they may have focal capsular (when encapsulated) or focal peripheral (if circumscribed but unencapsulated) infiltration. The latter group of *RAS*-driven or *RAS*-like driven tumors are akin to follicular thyroid carcinomas. Hence, as per the recent WHO guidelines, five of the predominantly macrofollicular cases with evidence of infiltration in the series by Albores-Saavedra would have been characterized as IEFVPTC, and the majority would have been NIFTP.

The issue for malignant tumors with predominantly macrofollicular architecture is that they are often unnoticed, especially as a component of thyroid follicular nodular disease. The abundant colloid flattens the follicular cells making PTC-N virtually inapparent [3]. The difficulty in histopathological diagnosis of macrofollicular NIFTP/IEFVPTC reflects in the cytologic and radiologic evaluation of these nodules, too. Owing to the rarity and likely under-recognition of these lesions, especially given the predominantly favorable outcomes following surgery, the cytological [4], radiological [5] and gross tumor appearance [6–9] of these tumors are not well characterized. Here, we report a comprehensive description of the radiological, cytological, gross, microscopic and molecular features of a small series of four such cases seen at our institute over the past two years. A review of the available literature along with diagnostic pitfalls is also discussed.

Materials and Methods

Between 2021 and 2022, 946 thyroid specimens were received for histopathology examination in the department of Pathology, All India Institute of Medical Sciences, New Delhi. Of these, 208 (22%) were PTC, including 45 FVPTC. Among the latter, there were 36 IEFVPTC and 9 invasive. Of the IEFVPTC, four showed a predominantly (> 50% of tumor area) macrofollicular architecture with follicles measuring > 200 μm in diameter, diagnostic PTC-N, and lacked true papillae [1]. The cases were reviewed by endocrine pathologists (SA, MCS). Patients were staged in accordance with the 8th edition of the American Joint Committee on Cancer (AJCC) [10]. The pre-operative thyroid ultrasound images, fine needle aspirate (FNA) smears and images of the resection specimens were retrieved.

A specialist (DK) re-assessed the radiology dataset for the following parameters: nodule composition, echogenicity, shape, margin, echogenic foci, halo, echotexture and the ACR TI-RADS (American College of Radiology Thyroid Imaging Reporting & Data System) score.

The cytology preparations included direct smears stained with May-Grunwald Giemsa and Papanicolaou stains. The slides were analyzed by two pathologists (SA, SY) for cellularity, presence and nature of colloid, architecture, nuclear characteristics, and the presence of any other findings like resorption vacuoles, giant cells, cyst macrophages, and oncocytic cells.

Molecular analysis was performed using DNA extracted from formalin-fixed, paraffin-embedded tumor tissue for the hotspot thyroid carcinoma-associated mutations involving *BRAF*, *KRAS*, *NRAS*, and *HRAS* genes. The EntroGen thyroid mutation analysis kit (THDNA-RT64, Entrogen Inc, CA, USA) was used for the purpose. The kit includes 5 primer mixes: first for detecting *BRAF* V600E, second for *KRAS* p.G12A/D/R/V, *KRAS* p.G13D, third for *KRAS* p.G12C/S, fourth for *NRAS* p.Q61H/L/K/R, and fifth for *HRAS* p.G12V, *HRAS* p.G13R, *HRAS* p.Q61R. The detailed protocol of the allele-specific real-time polymerase chain reaction (PCR) has been previously described elsewhere [11]. Formalin-fixed, paraffin-embedded sections from tumors that were negative for the above mutations were evaluated for *ETV6::NTRK3* fusion by dual fusion fluorescence in situ hybridization (FISH) probes (#CT-PAC245-10-OG; CytoTest Inc., USA). Four-micrometer sections were deparaffinized in xylene and dehydrated in ethanol. After air-drying at room temperature, slides were dipped in Pretreatment (PT)-1 buffer (#PS021-CC, BioMarq) at 98 °C for 1 h, followed by a 5-min wash in saline sodium citrate (SSC) buffer (#V4261, Promega) and then in MQ water. 1 mg/mL of pepsin (#P7012-1G, Sigma Aldrich) was used for digestion at 37 °C followed by washing using SSC buffer and MQ water (3 min each). Dehydration of the tissue samples was done by passing through increasing grades of ethanol. The probe mixture (5 μl per slide) was applied to the region of interest. Probe/specimen denaturation was performed at 77 °C for 5 min with subsequent overnight incubation at 37 °C in a hybridization chamber (ThermoBrite StatSpin, Abbott Molecular). The sections were washed the next day in 2X SSC (2 min at 73 °C) followed by 2X SSC (2 min at room temperature) and counterstained with 4,6-diamidino-2-phenylindole (DAPI) (#CT-ACC004-20-D, CytoTest Inc., USA) and visualized under a fluorescence microscope (Zeiss Axio Imager.D2; Carl Zeiss microscopy). Signals were scored at least in 100 non-overlapping intact nuclei, and the number of test signals (orange and green) was noted. Cases with $\geq 30\%$ nuclei showing fusion of red and green signals were considered harboring *ETV6::NTRK3* fusion. The remaining tumors lacking *NTRK* fusion were further assessed for *RET* fusions using break-apart probes (#CT-PAC051-10-OG; CytoTest Inc., USA). Two immediately adjacent red/green signals or a fused yellow signal indicate intact *RET*. Cases with at least 7.6% of cells displaying

split signals \geq two signal diameters between the 5' and 3' signals and/or single 3' (green) patterns were considered *RET* fusion-positive [12].

The patients were followed-up in the Department of Nuclear Medicine with I-131 whole-body planar scintigraphy, serum thyroglobulin (TG) levels and anti-Tg antibodies. Where appropriate, they were administered therapeutic radioactive iodine (RAI). Treatment response was defined per the American Thyroid Association (ATA) guidelines as Excellent response: negative imaging, absent anti-Tg antibodies, and either suppressed Tg < 0.2 ng/mL or TSH stimulated Tg < 1 ng/mL; Biochemically incomplete response: negative imaging, and suppressed Tg ≥ 1 ng/mL or stimulated Tg ≥ 10 ng/mL in the absence of anti-Tg antibodies or rising anti-Tg antibody levels; Structurally incomplete response: Structural or functional evidence of disease with any Tg level with or without anti-Tg antibodies; Indeterminate response: Nonspecific findings on imaging studies, faint uptake in thyroid bed on RAI scanning, non-stimulated Tg detectable but < 1 ng/mL, stimulated

Tg detectable but < 10 ng/mL, or anti-Tg antibodies stable or declining in the absence of structural or functional disease [13].

Results

Patient Demographics

Table 1 provides the clinical details along with a summary of the radiology, cytology, histopathology and molecular findings. The median age of the patients was 27 years (range 21–33 years). There were two males and two females. The duration of the disease ranged from 1 to 10 years (median, 6 years).

Ultrasound Features

The thyroid ultrasound findings were available for review in three patients and have been detailed in Table 2 and Fig. 1.

Table 1 Clinical, radiology, cytology, histopathology and molecular findings of the cases

Parameters	Case 1	Case 2	Case 3	Case 4
Age (years)	21	32	22	33
Sex	Female	Female	Male	Male
Duration of disease	10 years	10 years, rapid size increase over 6 months	2 years	1 year
Tumor size (cm)	10	11.5	6	5
Laterality	Left lobe	Right lobe	Left lobe	Left lobe
Thyroid USG: ACR-TIRADS score	TR4 (Moderately suspicious)	TR1 (Benign)	TR2 (Not suspicious)	NA
Cytology	Bethesda I	Bethesda III	Bethesda II	NA
Primary surgical procedure	Left hemithyroidectomy	Right lobectomy	Left hemithyroidectomy	Left hemithyroidectomy
Second surgery	None	Completion thyroidectomy and right neck lymph node dissection; associated papillary microcarcinoma	Completion thyroidectomy; normal thyroid	None
Extrathyroidal extension	Absent	Absent	Absent	Absent
Lymph node metastases	Present (central compartment)	Present (central compartment & right Level IV)	Absent	Absent
Distant metastases	Lung	Lung, bone	None	None
Adjoining thyroid	Normal thyroid	Thyroid follicular nodular disease	Normal thyroid	Lymphocytic thyroiditis
AJCC Stage (8 th edition)	pT3aN1aM1 (II)	pT3aN1bM1 (II)	pT3aN0M0 (I)	pT3aN0M0 (I)
Molecular	None	<i>NRAS</i> mutation	None	<i>ETV6::NTRK3</i>
Radioactive iodine	150 mCi followed 6 months later by 120 mCi	150 mCi followed 6 months later by 200 mCi	Single dose of 30 mCi	Single dose of 30 mCi
Follow-up	12 months: Structurally incomplete response	12 months: Structurally incomplete response	6 months: Indeterminate response	6 months: Excellent response

ACR TI-RADS American College of Radiology Thyroid Imaging Reporting & Data System, AJCC American Joint Committee on Cancer; Ki-67 LI: Ki-67 labelling index, NA not applicable/available; USG ultrasonogram

Table 2 Thyroid ultrasonographic characteristics of the cases

Parameters	Case 1	Case 2	Case 3
Composition	Solid-cystic	Predominantly cystic	Solid-cystic
Echogenicity	Isoechoic	Hypoechoic	Isoechoic
Shape	Wider	Wider	Wider
Margin	Smooth	Smooth	Smooth
Echogenic foci	Microcalcifications	None	None
Halo	Complete	None	Incomplete
Echotexture	Heterogeneous	Homogeneous	Homogeneous
ACR TI-RADS score	TR4 (Moderately suspicious)	TR1 (Benign)	TR2 (Not suspicious)

ACR TI-RADS American College of Radiology Thyroid Imaging Reporting & Data System

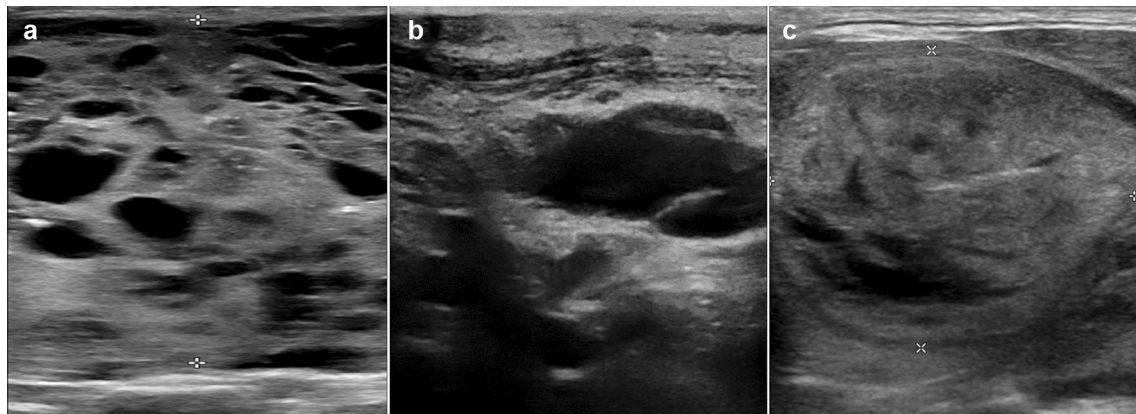


Fig. 1 Thyroid Ultrasound images of the cases: **a** Case 1- a solid-cystic lesion having focal spongiform pattern and scattered microcalcifications. **b** Case 2- a predominantly cystic lesion with few septations, lacking high-risk features. **c** Case 3- a solid-cystic lesion that

is isoechoic with the surrounding thyroid parenchyma and having an incomplete halo. The lesion is wider than tall and does not show any high-risk features

While case 1 was TR4 (moderately suspicious), the others were TR1 (benign) or TR2 (not suspicious). Extrathyroidal extension was absent in all.

Cytological Features

Aspiration cytology smears were available in three cases, of which one (Case 1) showed only thin colloid and cyst macrophages. Being a TR4 nodule, the aspirate was considered nondiagnostic. Aspirate from Case 2 showed follicular cells arranged as honeycomb sheets and tight 3-dimensional fragments in a colloid-rich background. Although the nuclei were predominantly round, there was focal elongation and occasional nuclear grooves, leading to a diagnosis of atypia of undetermined significance (Fig. 2a, b; Table 3). Case 3 was moderately cellular and had a hemorrhagic background. The cells were arranged as loose clusters with scattered microfollicles. The nuclei were predominantly round and minimally enlarged. Grooves were rare. The case was categorized as benign (Fig. 2c, d; Table 3). In Case 4, the

aspirate was performed in a private laboratory and reported as a colloid nodule, with many benign follicular cells, colloid and hemosiderin-laden macrophages. The smears were not available for review.

Macroscopic, Histopathological and Molecular Findings

Gross macroscopic (formalin-fixed) images were available for Cases 1, 2 and 3. The tumors varied in size from 5 to 11.5 cm, were solid-cystic, and showed variable amounts of colloid. While Case 1 had a unique spongiform appearance (Fig. 3a), Case 2 had nodular growth (Fig. 3b). Case 3 had abundant colloid on the surface mimicking thyroid follicular nodular disease (Fig. 3c). At least one section per centimeter of the tumor was processed for microscopy, with number of sections being ten, thirty-one and twelve for Cases 1, 2, and 3, respectively. These sections included the periphery and the center of the tumor. Case 4 had been grossed at a private laboratory

Fig. 2 Cytological features of the cases: **a** A tight fragment of follicular epithelial cells along with cyst macrophages (arrow) in a colloid-rich background (400X, May Grunwald-Giemsa; case 2). **b** A sheet of follicular cells showing nuclear crowding, focal elongation and occasional grooves (400X cropped and enlarged, May Grunwald-Giemsa; case 2). **c** Dyscohesive clusters of follicular cells having round but mildly enlarged nuclei (200X, May Grunwald-Giemsa; case 3). **d** Follicular cells arranged as microfollicles and dyscohesive clusters having round, mildly enlarged nuclei with minimal overlapping (400X cropped and enlarged, May Grunwald-Giemsa; case 3)

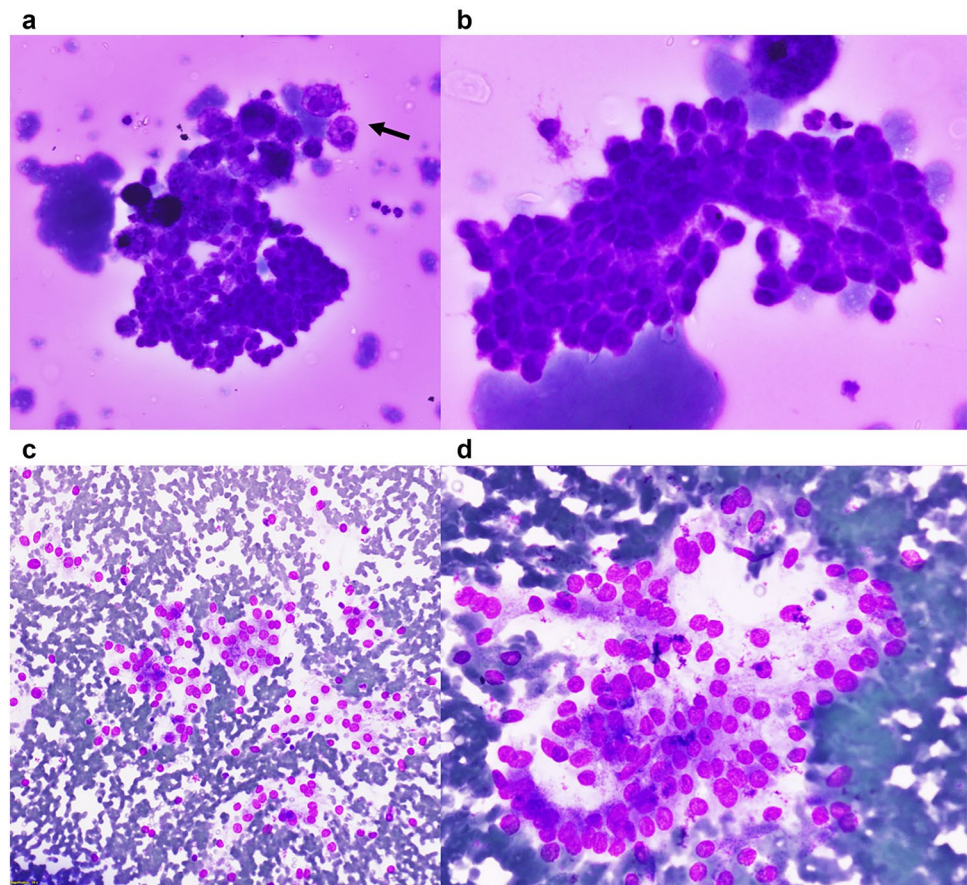


Table 3 Cytological features of cases

Parameters	Case 1	Case 2	Case 3
Cellularity	None	Low	Moderate
Architecture	–	Honeycomb sheets, tight fragments	Dyscohesive clusters, microfollicles
Nuclear shape	–	Round, focal elongation	Round
Nuclear overlap/crowding	–	Present, focal	Present, minimal
Nuclear enlargement	–	Mild	Mild
Nuclear grooves/membrane irregularity	–	Present, focal	Rare groove
Pseudoinclusions	–	Absent	Absent
Oncocytic change	–	Absent	Absent
Multinucleate giant cells	–	Absent	Absent
Chromatin	–	Fine granular	Fine granular
Nucleolus	–	Absent	Absent
Colloid	Thin, abundant	Thin and thick, abundant	Absent
Cyst/ hemosiderin-laden macrophages	Few	Many	Many
Other findings	–	Resorption vacuoles	–
Bethesda category	Nondiagnostic (I)	Atypia of undetermined significance, nuclear atypia (III)	Benign (II)

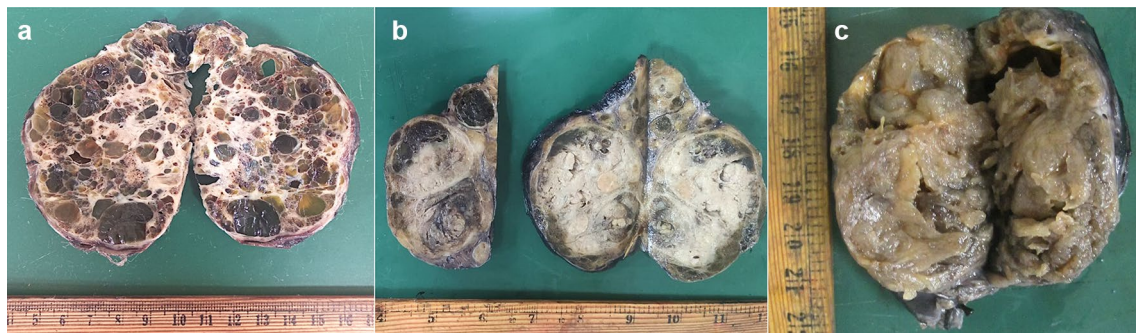


Fig. 3 Macroscopic features of the cases: **a** Spongy gross appearance with large colloid-filled cysts of variable sizes, separated by fibrous septae (Case 1), **b** A multinodular tumor showing large colloid-filled cysts and solid grey-white haemorrhagic areas (Case 2), **c** A large

nodular and heterogeneous tumor. The nodules have a glistening, translucent cut-surface due to abundant colloid, resembling thyroid follicular nodular disease (Case 3)

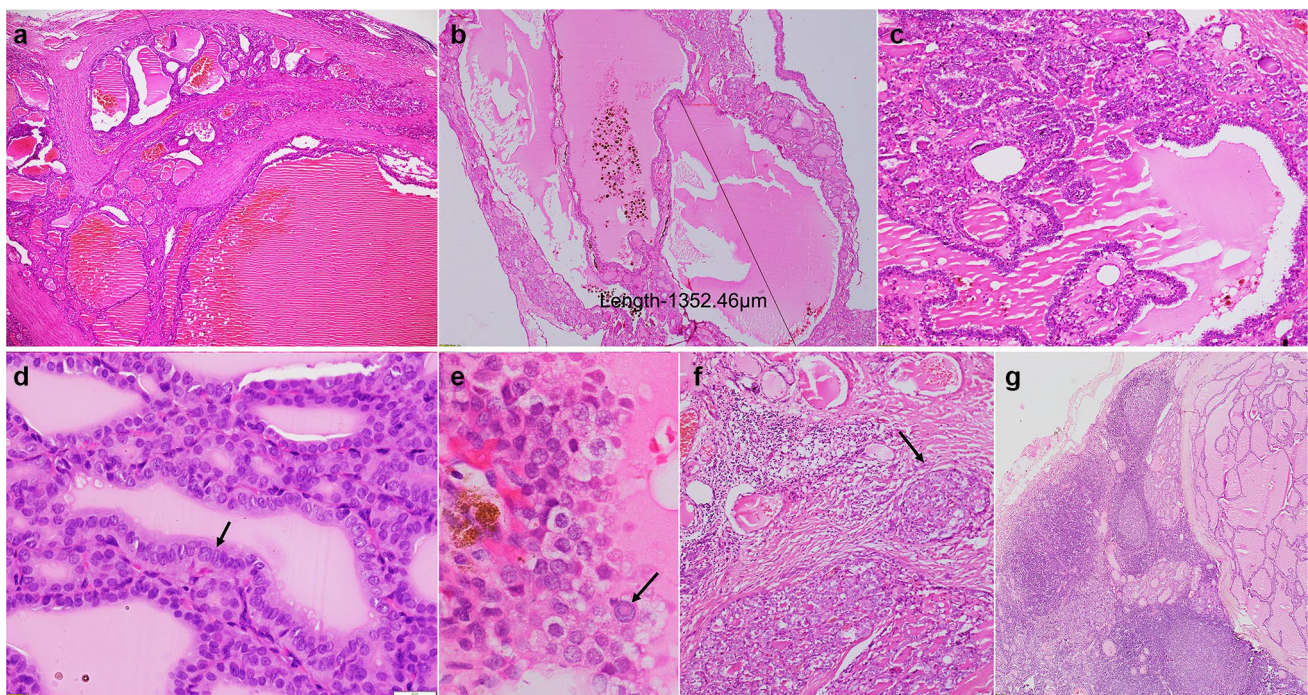


Fig. 4 Histopathological features of the cases: **a** Multinodular growth pattern with tumor nodules separated by fibrous septae (40X, Hematoxylin & Eosin; Case 4), **b** Microscopic image depicting a macrofollicle measuring 1352.46 μm (40X, Hematoxylin & Eosin; Case 3), **c** Focal pseudopapillary arrangement of tumor cells (100X, Hematoxylin & Eosin; Case 4), **d** Diagnostic nuclear features of PTC including elongation, crowding, overlapping, chromatin clearing and occa-

sional grooves, more evident in central portion of the image (arrow) (400X, Hematoxylin & Eosin; Case 3), **e** Predominantly round nuclei but prominent intranuclear inclusion in case 1 (arrow) (400X, Hematoxylin & Eosin; Case 1), **f** Nodular infiltrative edge of tumor (arrow) (100X, Hematoxylin & Eosin; Case 4), **g** Lymph node with metastatic disease (40X, Hematoxylin & Eosin; Case 2)

and four tumor blocks were available for review. Microscopically, all tumors were at least partially encapsulated and showed a multinodular growth pattern, with nodules separated by fibrous septae (Fig. 4a). Within the nodules, tumor cells were arranged as colloid-filled macrofollicles (Fig. 4b) with interspersed microfollicles. Tumors showed scalloping of colloid and pseudopapillary infoldings into the macrofollicles (Fig. 4c), mimicking thyroid follicular

nodular disease. Case 1, in addition, showed focal non-psammomatous calcification, and Case 4 had small foci of oncocyctic metaplasia with occasional psammoma bodies. All cases had predominantly round nuclei but there was conspicuous nuclear enlargement, prominent chromatin clearing and patchy nuclear membrane irregularities with associated nuclear grooves (Fig. 4d). Pseudoinclusions were well-developed and diffuse in Case 1 (Fig. 4e). In

Case 4, these were rare and found in the foci of oncocytic metaplasia. None were noted in Cases 2 and 3. Increased mitoses ($\geq 5/2\text{mm}^2$) and necrosis were absent in all. Instead of mushrooming-type infiltration, the tumors showed nodular infiltration into the adjacent thyroid parenchyma (Fig. 4f). Angioinvasion was absent in all.

Case 1 and Case 2 had cervical lymph node metastases. Case 1 had metastases involving the central compartment dissected during the primary surgery. In Case 2, nodal disease involved the right lateral and central compartments and was removed during the second-stage surgery. The metastases had similar histomorphology to the primary tumor. There was a predominantly macrofollicular architecture with fewer microfollicles and absent papillae (Fig. 4g).

Molecular studies revealed *NRAS* mutation in Case 2. Both the primary tumor and the lymph node metastasis harbored the mutation. *ETV6::NTRK3* fusion was detected in Case 4. All the assessed cases showed normal *RET* patterns (Fig. 5).

Follow-up

Hematogenous metastases were noted in Cases 1 (lung) and 2 (lung, bone) on I-131 whole-body iodine planar scintigraphy performed 47 days and 73 days after primary surgery, respectively (Table 1). Therapeutic RAI was administered to all four patients (Table 1). While Cases 1 and 2 had a structurally incomplete response at 12 months, Case 4 had an excellent response at 6 months. Case 3 showed no residual/recurrent disease at 6 months but the stimulated thyroglobulin level was 7.0 ng/mL (indeterminate response).

Discussion

In thyroid, macrofollicular architecture is typically associated with benign pathology, particularly thyroid follicular nodular disease. Rarely, it may be seen as the predominant architecture in PTC or follicular thyroid carcinoma [1]. Such cases pose a diagnostic challenge at all tiers of patient evaluation [14]. The macrofollicular variant (previously a unique subtype of PTC) was first described by Albores-Saavedra in 1991 [1]. Since then, various authors have published their experience as case reports or series [5, 6, 9, 14–18], the largest based on a cohort of 11 patients [14]. The 2022 WHO classification no longer recognizes the macrofollicular variant as a distinct subtype of PTC. Instead, a macrofollicular arrangement of cells has been included among architectural patterns in NIFTP, well-differentiated thyroid tumors of uncertain malignant potential (WDT-UMP), IEFVPTC, follicular thyroid adenoma and follicular thyroid carcinoma [2]. Additionally, only those encapsulated follicular-patterned cases that have invasive features besides PTC-N can now be called ‘carcinoma’ [2]. Hence, all the previous studies on macrofollicular PTC, based solely on the diagnostic criteria laid down by Albores-Saavedra [1], likely included NIFTP and WDT-UMP.

Thyroid Ultrasound

Macrofollicular lesions lack the typical ultrasound findings associated with PTC. Although a few authors have detailed thyroid ultrasound findings in patients with macrofollicular thyroid tumors [5, 7, 14] none have provided a TI-RADS score for those associated with malignancy. Of the five cases studied by Fukushima, two were characterized as benign on ultrasound and three as suspicious [7]. PTC are typically

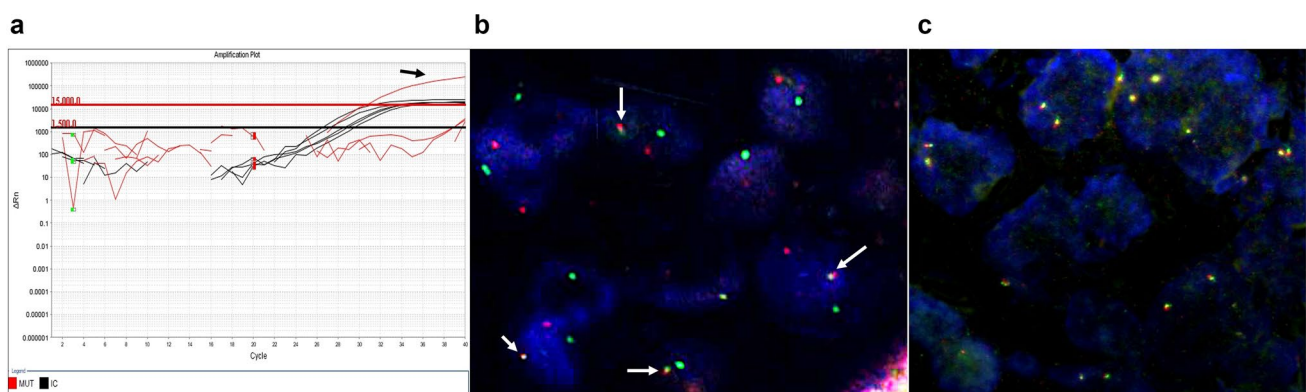


Fig. 5 Molecular characteristics of the cases: **a** Graph showing *NRAS* mutation in case 2 (arrow), as detected by allele-specific real-time polymerase chain reaction, **b** Fluorescence in situ hybridization assay, performed using dual fusion probes, showing *ETV6::NTRK3* gene

fusion as depicted by fused green and red signals in case 4 (arrows), **c** Fluorescence in situ hybridization assay, performed using break-apart probes, showing two fused red and green signals per nucleus, indicating lack of *RET* gene rearrangements (case 3)

solid, markedly hypoechoic, taller than wide on transverse view, and have micro and/or macrocalcifications, and irregular margins with an absent halo. In contrast, most cases of IEFVPTC are solid, hypo or isoechoic, wider than tall, and have a round to oval shape, smooth margins, and a halo. Following the ATA guidelines, such lesions get categorized as ‘intermediate suspicion of malignancy’ [19]. Our cases had similar findings except for being solid-cystic, spongiform or predominantly cystic. These latter features contribute to low TI-RADS scores yielding misclassification as low suspicion, very low suspicion, or benign nodules [20]. Owing to their macrofollicular architecture, the spongiform ultrasound appearance typical of thyroid follicular nodular disease may be seen in a predominantly macrofollicular PTC [14], as seen in case 1 (Fig. 1a).

Cytomorphological Features

Predominantly macrofollicular IEFVPTC is often mischaracterized on FNA cytology as benign (Bethesda II) or indeterminate (Bethesda III or IV) [9]. This is because the cytology preparations from predominantly macrofollicular PTC are usually sparsely cellular, have abundant colloid, show an admixture of macro- and microfollicles, are frequently cystic with hemosiderin-laden macrophages, and lack papillae and psammoma bodies. Also, nuclear features are more commonly ill-developed [9, 21], focal and not noted in most cytological preparations [15]. The nuclei are mildly enlarged and predominantly round/ovoid rather than elongated. Chromatin clearing, nuclear overlapping and nuclear grooves are often patchy and variable. A review of cytology findings across published articles revealed intranuclear inclusions to be rare or few and present in 45% of the 24 cases assessed. Other prominent findings include moderate to abundant thin and thick colloid in 75% and sheet-like arrangement of cells in 76% [22]. Hence, on cytology, only those cases that show PTC-N, especially with intranuclear inclusions, are classified preoperatively as PTC. Yeo reviewed the data of 71 patients of cases previously classified as macrofollicular variant of PTC [9]. Of the 35 with available cytology findings, a third (37%) were diagnosed as PTC on cytology. The rest of the categories included benign (29%), atypia of undetermined significance (20%) and follicular neoplasm (14%) [9]. In the current study, there was abundant colloid in two cases, and nuclear features were absent to very subtle, leading to categorization of the cases as nondiagnostic, benign, or indeterminate.

Gross (Macroscopic) Features

There is sparse literature on the gross/macroscopic appearance of malignant macrofollicular thyroid tumors. Our cases were circumscribed and partly encapsulated, variably

solid and cystic, akin to their ultrasonographic findings. The spongy cut surface in Case 1 was unique, and we could not make a gross diagnosis on this specimen. In retrospect, it can be explained by the presence of a prominent cystic component composed of many large colloid-filled cysts. The appearance corroborated with the ultrasound that had been independently assessed by the radiologist as focally spongiform. Previous reports have described the cut surfaces as nodular [8] and “succulent” [7, 9]. Extrathyroidal extension has been reported in about 12% of these previously reported cases [9], but since the publication of several of these reports, the definition of extrathyroidal extension has been modified to only consider macroscopic extrathyroidal extension [10]. No such findings were observed in the current cohort.

Histomorphological and Molecular Features

All cases described herein were partly encapsulated with nodular infiltrative growth in a pattern distinct from typical mushrooming invasion associated with IEFVPTC. Multinodular infiltrative tumor growth has been previously described [6, 8, 14]. The pseudopapillary infoldings into follicles is also a prominent feature. Similar to IEFVPTC, PTC-N may be focal and ill-developed. Nuclei are more likely to be round, showing patchy elongation and grooves. Chromatin clearing was present in all but pseudoinclusions were found in only two of the four cases.

Two other studies have analyzed the molecular profile of tumors previously described as macrofollicular variant of PTC [9, 23]. Using PCR amplification and DNA sequencing, Yeo did not find any molecular alteration involving the *BRAF* codons 600–601, *NRAS* codon 61, *HRAS* codon 61, and *KRAS* codons 12–13 and 61 in their two samples [9]. *BRAF* exon 11 and 15 alterations were absent in one other case assessed by Puztaszeri [23]. A prior study had shown all six of their tumors to be diploid [24]. Of our four cases, one harbored *NRAS* codon 61 mutation and another *ETV6::NTRK3* fusion.

In a prior work, *ETV6::NTRK3*-translocated PTC were found to show a multinodular growth pattern in 50%, mixed follicular and papillary arrangement of cells and associated chronic lymphocytic thyroiditis in two-thirds. The nuclear features were well-developed but patchy with intervening areas having bland nuclei. Cytoplasmic vacuolization, psammoma bodies and oncocytic metaplasia were also noted [25]. Since then, a number of studies have reported on the morphology of *NTRK* fusion-related thyroid carcinomas [26] as well as other tyrosine kinase-related thyroid carcinomas [27, 28], including cytological features [29]. Case 4 with *NTRK3* fusion showed most of these features.

There are some limitations concerning the molecular work-up in the current series. We did not assess for

DICER1 mutations reported in the macrofollicular subtype of follicular thyroid carcinoma [30]. None of the cases had any clinical or family history indicative of *DICER1* syndrome. However, spontaneous *DICER1* mutations have been reported in follicular-patterned thyroid carcinomas [31]. Two of our cases had distant metastases, but unfortunately, given resource constraints, further genetic work-up, including for *TERT* promoter mutations, was not performed. Next-generation sequencing will help in better elucidation of the molecular pathways involved in these tumors, and any additional molecular alterations that may be present and influence clinical outcome.

Clinical Outcome

In the current study, two of the four cases had an aggressive outcome with lymphatic and hematogenous metastatic disease. However, notwithstanding the findings in our cases, most tumors with predominantly macrofollicular growth demonstrate indolent behavior, with only single reports of adverse outcomes having been associated with macrofollicular-patterned carcinomas [4, 32]. In Yeo's meta-analysis, which showed 7% of historical cases to be associated with distant metastasis and 26% with lymph node metastases, no genetics were performed, and none of these cases were re-reviewed to affirm classification. Hence, these cohorts of cases, at least cases with metastases, need to be revisited prior to drawing definitive conclusions [9]. Further, since most authors did not report evidence of recurrent disease over a follow-up period ranging from two months to 23 years, it is safe to conclude that this disease process is overtly indolent [9]. Although the proportion of cases with aggressive presentation in our series is high, our series consists of only four cases from a tertiary care referral center, and there may be a selection bias. Moreover, previous studies may have included cases that would currently be classified as NIFTP, WDT-UMP, or even classic PTC with predominantly follicular architecture, likely to be positive for *BRAF* p.V600E, especially those with metastatic disease, and for cases negative for *BRAF* p.V600E, fusion kinase-related carcinomas is a possibility, especially given their architecture [27].

Conclusions

The diagnosis of invasive encapsulated follicular variant of PTC with predominantly macrofollicular architecture is difficult, especially given the preoperative, gross (macroscopic) and microscopic tendencies to discount macrofollicular thyroid tumors as being worrisome for malignancy. Long-standing disease, overlapping pathology with benign diseases, and lack of diagnostic ultrasonographic and cytological

characteristics make it more likely to be underdiagnosed/misclassified during pre-operative work-up.

Although our study had a limited duration of follow-up, the documentation of metastatic disease and incomplete response to radioactive iodine, even in our limited cohort, underscores the need for increased awareness of malignancy in macrofollicular neoplasia with enhanced molecular correlates needed given the above-mentioned diagnostic caveats. Here, we report the macroscopic (gross) spongy appearance and the presence of *NRAS* mutations and *ETV6::NTRK3* fusion in these rare tumors. Potential review of prior macrofollicular cohorts with metastatic disease should be considered to assess for molecular drivers.

Author Contributions Conceptualization: SA; methodology: SA, SY, MCS, DK, ND, RG; writing—original draft preparation: SY, SA; writing—review and editing: SA, SY, MCS, DK, ND, RG, SC; resources: SA, DK, ND, SC, MB; supervision: SA.

Funding This study was not supported by any funding.

Declarations

Conflict of interest The authors declare that they have no conflict of interest.

Ethical Approval For this type of study formal consent is not required.

Informed Consent For this type of study formal consent is not required.

Consent for Publication For this type of study consent for publication is not required.

References


- Albores-Saavedra J, Gould E, Vardaman C, Vuitch F (1991) The macrofollicular variant of papillary thyroid carcinoma: a study of 17 cases. *Hum Pathol* 22:1195–1205. [https://doi.org/10.1016/0046-8177\(91\)90101-t](https://doi.org/10.1016/0046-8177(91)90101-t)
- Baloch ZW, Asa SL, Barletta JA, Ghossein RA, Juhlin CC, Jung CK, LiVolsi VA, Papotti MG, Sobrinho-Simões M, Tallini G, Mete O (2022) Overview of the 2022 WHO Classification of Thyroid Neoplasms. *Endocr Pathol* 33:27–63. <https://doi.org/10.1007/s12022-022-09707-3>
- Albores-Saavedra J, Wu J (2006) The many faces and mimics of papillary thyroid carcinoma. *Endocr Pathol* 17(1):1–18. <https://doi.org/10.1385/ep:17:1:1>
- Lugli A, Terracciano LM, Oberholzer M, Bubendorf L, Tornillo L (2004) Macrofollicular variant of papillary carcinoma of the thyroid. *Arch Pathol Lab Med* 128:54–58. <https://doi.org/10.5858/2004-128-54-MVOPCO>
- Lee YS, Kim SY, Hong SW, Kim SM, Kim BW, Chang HS, Park CS (2018) Ultrasonographic features and clinicopathologic characteristics of macrofollicular variant papillary thyroid carcinoma. *Medicine* 97:e8105. <https://doi.org/10.1097/MD.00000000000008105>
- Candanedo-Gonzalez F, Rodriguez-Orihuela D, Arista-Nasr J (2020) Macrofollicular variant of papillary thyroid carcinoma

- with metastasis to femur. *Thyroid Res* 13:10. <https://doi.org/10.1186/s13044-020-00083-w>
7. Fukushima M, Ito Y, Hirokawa M, Kobayashi K, Miya A, Takamura Y, Akasu H, Shimizu K, Miyauchi A (2009) Macrofollicular variant of papillary thyroid carcinoma: its clinicopathological features and long-term prognosis. *Endocr J* 56:503–508. <https://doi.org/10.1507/endocrj.k08e-346>
 8. Emad R, Maha A, Kfoury HK, Al-Sheikh AM, Zaidi SN (2011) Three cases of macrofollicular variant of papillary thyroid carcinoma. *Ann Saudi Med* 31:644–647. <https://doi.org/10.4103/0256-4947.87104>
 9. Yeo MK, Bae JS, Oh WJ, Park GS, Jung CK (2014) Macrofollicular variant of papillary thyroid carcinoma with extensive lymph node metastases. *Endocr Pathol* 25:265–272. <https://doi.org/10.1007/s12022-014-9306-y>
 10. Tuttle M, Morris LF, Haugen B, Shah J, Sosa JA, Rohren E, Subramaniam RM, Hunt JL, Perrier ND (2017) Thyroid-differentiated and anaplastic carcinoma. In: Amin MB, Edge SB, Greene F, Byrd D, Brookland RK, Washington MK, Gershenwald JE, Compton CC, Hess KR, Sullivan DC, Jessup JM, Brierley J, Gaspar LE, Schilsky RL, Balch CM, Winchester DP, Asare EA, Madera M, Gress DM, Meyer LR (eds) *AJCC cancer staging manual*, 8th edn. Springer, New York, pp 873–901
 11. Boruah M, Gaddam P, Agarwal S, Mir RA, Gupta R, Sharma MC, Deo SV, Nilima N (2023) PD-L1 expression in rare and aggressive thyroid cancers: A preliminary investigation for a role of immunotherapy. *J Cancer Res Ther* 19:312–320. https://doi.org/10.4103/jcrt.jcrt_1471_22
 12. Liu Y, Wu S, Zhou L, Guo Y, Zeng X (2021) Pitfalls in RET fusion detection using break-apart FISH probes in papillary thyroid carcinoma. *J Clin Endocrinol Metab* 106:1129–1138. <https://doi.org/10.1210/clinem/dgaa913>
 13. Haugen BR, Alexander EK, Bible KC, Doherty GM, Mandel SJ, Nikiforov YE, Pacini F, Randolph GW, Sawka AM, Schlumberger M, Schuff KG, Sherman SI, Sosa JA, Steward DL, Tuttle RM, Wartofsky L (2016) 2015 American Thyroid Association Management Guidelines for Adult Patients with Thyroid Nodules and Differentiated Thyroid Cancer: The American Thyroid Association Guidelines Task Force on Thyroid Nodules and Differentiated Thyroid Cancer. *Thyroid* 26:1–133. <https://doi.org/10.1089/thy.2015.0020>
 14. Ng SC, Huang BY, Kuo SF, Hsueh C, Chiang KC, Chen CH, Lin JD (2019) Diagnostic pitfalls and therapeutic outcomes of the macrofollicular variant of papillary thyroid carcinoma. *Biomed J* 42:59–65. <https://doi.org/10.1016/j.bj.2018.12.006>
 15. Raddaoui E (2015) Macrofollicular variant of papillary thyroid cancer: a clinicopathologic and molecular review. *Int J Endocrinol Metab* 13:e16538. <https://doi.org/10.5812/ijem.16538>
 16. Erol V, Makay O, Ertan Y, İçöz G, Akyıldız M, Yılmaz M (2014) Papillary thyroid cancer, macrofollicular variant: the follow-up and analysis of prognosis of 5 patients. *J Thyroid Res* 2014:818134. <https://doi.org/10.1155/2014/818134>
 17. Qichun Y, Jinguang Y, Yanhong S, Weihua Q, Jian T (2018) Macrofollicular variant of papillary thyroid carcinoma: a report of 3 cases. *J Surg Concepts Pract* 23:57–61. <https://doi.org/10.16139/j.1007-9610.2018.01.013>
 18. Saleem N, Bajaj NK, Nagamuthu EA (2021) Cytohistological concordance of papillary carcinoma of thyroid and its variants. *J Evid Based Med Healthc* 8:213–218. <https://doi.org/10.18410/jebmh/2021/41>
 19. Hahn SY, Shin JH, Oh YL, Kim TH, Lim Y, Choi JS (2017) Role of Ultrasound in predicting tumor invasiveness in follicular variant of papillary thyroid carcinoma. *Thyroid* 27:1177–1184. <https://doi.org/10.1089/thy.2016.0677>
 20. Tang AL, Falciglia M, Yang H, Mark JR, Steward DL (2017) Validation of American Thyroid Association ultrasound risk assessment of thyroid nodules selected for ultrasound fine-needle aspiration. *Thyroid* 27:1077–1082. <https://doi.org/10.1089/thy.2016.0555>
 21. Chung D, Ghossein RA, Lin O (2007) Macrofollicular variant of papillary carcinoma: a potential thyroid FNA pitfall. *Diagn Cytopathol* 35:560–564. <https://doi.org/10.1002/dc.20702>
 22. Policarpio-Nicolas MC, Sirohi D (2013) Macrofollicular variant of papillary carcinoma, a potential diagnostic pitfall: a report of two cases including a review of literature. *CytoJournal* 10:16. <https://doi.org/10.4103/1742-6413.117352>
 23. Pusztaszeri M, Auger M (2017) Update on the cytologic features of papillary thyroid carcinoma variants. *Diagn Cytopathol* 45:714–730. <https://doi.org/10.1002/dc.23703>
 24. Gamboa-Dominguez A, Vieitez-Martinez I, Barredo-Prieto BA, Richaud-Patin Y, Herrera ME, Angeles-Angeles A (1996) Macrofollicular variant of papillary thyroid carcinoma: a case and control analysis. *Endocr Pathol* 7:303–308. <https://doi.org/10.1007/BF02739837>
 25. Seethala RR, Chiosea SI, Liu CZ, Nikiforova M, Nikiforov YE (2017) Clinical and morphologic features of ETV6-NTRK3 translocated papillary thyroid carcinoma in an adult population without radiation exposure. *Am J Surg Pathol* 41:446–457. <https://doi.org/10.1097/PAS.0000000000000814>
 26. Chu YH, Dias-Santagata D, Farahani AA, Boyraz B, Faquin WC, Nosé V, Sadow PM (2020) Clinicopathologic and molecular characterization of NTRK-rearranged thyroid carcinoma (NRTC). *Mod Pathol* 33:2186–2197. <https://doi.org/10.1038/s41379-020-0574-4>
 27. Chu YH, Sadow PM (2022) Kinase fusion-related thyroid carcinomas: towards predictive models for advanced actionable diagnostics. *Endocr Pathol* 33:421–435. <https://doi.org/10.1007/s12022-022-09739-9>
 28. Chu YH, Wirth LJ, Farahani AA, Nosé V, Faquin WC, Dias-Santagata D, Sadow PM (2020) Clinicopathologic features of kinase fusion-related thyroid carcinomas: an integrative analysis with molecular characterization. *Mod Pathol* 33:2458–2472. <https://doi.org/10.1038/s41379-020-0638-5>
 29. Viswanathan K, Chu YH, Faquin WC, Sadow PM (2020) Cyto-morphologic features of NTRK-rearranged thyroid carcinoma. *Cancer Cytopathol* 128:812–827. <https://doi.org/10.1002/cncy.22374>
 30. Bongiovanni M, Sykietis GP, La Rosa S, Bisig B, Trimech M, Missiaglia E, Gremaud M, Salvatori Chappuis V, De Vito C, Sciarra A, Foulkes WD, Pusztaszeri M (2020) Macrofollicular variant of follicular thyroid carcinoma: a rare underappreciated pitfall in the diagnosis of thyroid carcinoma. *Thyroid* 30:72–80. <https://doi.org/10.1089/thy.2018.0607>
 31. Juhlin CC (2023) On the chopping block: overview of DICER1 mutations in endocrine and neuroendocrine neoplasms. *Surg Pathol Clin* 16:107–118. <https://doi.org/10.1016/j.path.2022.09.010>
 32. Cardenas MG, Kini S, Wisgerhof M (2009) Two patients with highly aggressive macrofollicular variant of papillary thyroid carcinoma. *Thyroid* 19:413–416. <https://doi.org/10.1089/thy.2008.0178>

Publisher's Note Springer Nature remains neutral with regard to jurisdictional claims in published maps and institutional affiliations.

Springer Nature or its licensor (e.g. a society or other partner) holds exclusive rights to this article under a publishing agreement with the author(s) or other rightsholder(s); author self-archiving of the accepted manuscript version of this article is solely governed by the terms of such publishing agreement and applicable law.

Authors and Affiliations

Sujata Yadav¹ · Devasenathipathy Kandasamy² · Nishikant Damle³ · Rashi Goel³ · Sunil Chumber⁴ ·
Mehar C. Sharma⁵ · Monikongkona Boruah¹ · Shipra Agarwal¹ 

✉ Shipra Agarwal
drshipra0902@gmail.com

Sujata Yadav
drsujata0505@gmail.com

Devasenathipathy Kandasamy
devammc@yahoo.co.in

Nishikant Damle
nkantdamle@gmail.com

Rashi Goel
dr.goelrashi@gmail.com

Sunil Chumber
sunil_chumber@hotmail.com

Mehar C. Sharma
sharmamehar@yahoo.co.in

Monikongkona Boruah
moni.boruah@gmail.com

¹ Department of Pathology, All India Institute of Medical Sciences, New Delhi, India

² Department of Radiodiagnosis, All India Institute of Medical Sciences, New Delhi, India

³ Department of Nuclear Medicine, All India Institute of Medical Sciences, New Delhi, India

⁴ Department of Surgical Disciplines, All India Institute of Medical Sciences, New Delhi, India

⁵ Department of Neuropathology, All India Institute of Medical Sciences, New Delhi, India